Substrate-induced antiferromagnetism of a Fe monolayer on the Ir(001) surface

Josef Kudrnovský,[1,2,*] František Máca,[1,2] Ilja Turek,[3] and Josef Redinger[4]
[1]*Institute of Physics ASCR, Na Slovance 2, CZ-182 21 Praha 8, Czech Republic*
[2]*Max-Planck Institut für Mikrostrukturphysik, Weinberg 2, D-06120 Halle, Germany*
[3]*Institute of Physics of Materials ASCR, Žižkova 22, CZ-616 62 Brno, Czech Republic*
[4]*Department of General Physics, Vienna University of Technology, Getreidemarkt 9/134, 1060 Vienna, Austria*
(Received 22 May 2009; revised manuscript received 20 July 2009; published 13 August 2009)

We present detailed *ab initio* study of structural and magnetic stability of a Fe monolayer on the fcc(001) surface of iridium. The Fe monolayer has a strong tendency to order antiferromagnetically for the true relaxed geometry. On the contrary an unrelaxed Fe/Ir(001) sample has a ferromagnetic ground state. The antiferromagnetism is thus stabilized by the decreased Fe-Ir layer spacing in striking contrast to the recently experimentally observed antiferromagnetism of the Fe/W(001) system which exists also for an ideal bulk-truncated, unrelaxed geometry. The calculated layer relaxations for Fe/Ir(001) agree reasonably well with recent experimental low-energy electron diffraction data. The present study centers around the evaluation of pair exchange interactions between Fe atoms in the Fe overlayer as a function of the Fe/Ir interlayer distance which allows for a detailed understanding of the antiferromagnetism of a Fe/Ir(001) overlayer. Furthermore, our calculations indicate that the nature of the true ground state could be more complex and display a spin spiral like rather than a $c(2\times 2)$-antiferromagnetic order. Finally, the magnetic stability of the Fe monolayer on the Ir(001) surface is compared to the closely related Fe/Rh(001) system.

DOI: 10.1103/PhysRevB.80.064405 PACS number(s): 75.30.−m, 81.20.−n

I. INTRODUCTION

Magnetic overlayers, i.e., the thin films of magnetic materials on the nonmagnetic substrate are systems with great technological potential. Magnetic overlayers are also a convenient system for a deeper understanding of the origin of magnetism in the solid state. The prototypical system is a magnetic monolayer (ML) on a nonmagnetic substrate which was the subject of many theoretical and experimental studies in the past.[1–13] Yet, a technological preparation, experimental study, and detailed theoretical understanding of the overlayer magnetism are still a challenge to solid-state physics.

There are a few important features which distinguish magnetic overlayers from conventional magnetic materials. This is, first of all, the presence of an external agent, namely, the presence of a nonmagnetic substrate, which can strongly modify the magnetic state and properties of the overlayer system: (i) the reduced coordination on the surface induces geometry as well as chemical binding changes. (ii) Magnetic atoms adapt to the underlying lateral substrate lattice spacings, particularly true for a monolayer case. (iii) The substrate electronic structure, in particular, the position of the substrate Fermi level is relevant for overlayer magnetism. (iv) The position of Fermi level can be tuned by the substrate electron concentration, e.g., by growing the overlayer on an alloy substrate with varying concentration of the constituents. Alternatively, one could consider a substrate alloy which contains magnetic and nonmagnetic species or only magnetic species, and/or a partial coverage of the substrate to vary the properties of the magnetic overlayer. Theoretical and experimental studies on the above trends help to establish a deeper understanding of the origin of surface magnetism.

First-principles calculations represent a powerful tool for such studies, as they allow to determine reliably the underlying lattice structure (possible layer relaxations, surface reconstructions, etc.) which can be directly compared with experiment [low-energy electron diffraction (LEED)]. They also allow to find out the underlying magnetic structure although in this respect the situation is much more complex. In addition to collinear magnetic configurations [ferromagnetic (FM) and antiferromagnetic (AFM) ones] more complex configurations may exist (e.g., recently observed chiral structures in bcc-Fe/W(001),[1] magnetism of random overlayers,[2] etc.). Consequently, an estimation and discussion of exchange interactions is very useful to gain a deeper understanding of properties of both overlayer and bulk magnets and magnetic alloys, including the diluted magnetic semiconductors.[14,15] Surprisingly and in contrast to bulk systems, studies of exchange interactions for magnetic overlayers are still very rare[3,4] despite of their obvious importance. In particular, the distance dependence of exchange integrals can be very different from that in the bulk if, for example, adatoms can interact via the host surface state as, e.g., Co adatoms on the fcc(111) faces on noble metals.[4,5]

Great emphasis, both theoretical and experimental, has been put recently on the study of the magnetic properties of Fe overlayers on the (001) and (110) faces of bcc tungsten. An unusual AFM state was predicted theoretically[7,8] and confirmed experimentally for the bcc-Fe/W(001) system[8] (in fact, the true ground state seems to be a more complex one exhibiting a chiral state[1]). There is also evidence from theory that the ground state of the Co/W(001) overlayer is AFM, whereas Mn and Cr overlayers have a FM ground state.[9] This means that a (Fe, Mn)-alloy overlayer on the bcc-W(001) should exhibit a crossover from an AFM to a FM ground state.[2] Finally, a similar AFM-to-FM crossover was predicted for the bcc-Fe/(Ta, W)(001) alloy substrate system,[10] where the ground state of the bcc-Fe/Ta(001) is FM. However, only the leading exchange integrals were estimated in the latter case.[10]

The (001) faces of the fcc and bcc substrates exhibit a simple rectangular array of lattice sites and differ essentially by the $d:a_L$ ratio, where a_L is the lateral lattice constant and d is the interlayer distance. Therefore an investigation of the magnetic properties of Fe overlayers on the (001) faces of fcc transition metals poses an interesting problem. A particularly suitable system is the fcc-Fe/Ir(001) where very thin overlayers were grown successfully with negligible Fe-Ir intermixing.[11] Furthermore, there exist reliable LEED measurements[11] elucidating the detailed geometry, while preliminary magneto-optic Kerr effect studies[11] indicate no magnetic signal in the limit of a monolayer coverage; a situation similar to the bcc-Fe/W(001).

The clean Ir(001) surface undergoes the (5×1) quasihexagonal reconstruction. The finite Fe coverage (larger than 0.25 ML) lifts the reconstruction.[11] In order to avoid possible corrugation and Fe-Ir intermixing the metastable unreconstructed (1×1)-Ir(001) surface was prepared which is, however, stable for room temperatures and below (for details see Ref. 11).

The aim of the present study is a comprehensive first-principles investigation of the properties of an fcc-Fe/Ir(001) monolayer system. In a first step we perform a structural study of Fe/Ir(001) by using two highly accurate DFT methods, namely, the WIEN2K (Ref. 16) and VASP (Refs. 17 and 18) codes. In the next step we investigate the magnetic structure of the geometrically relaxed system by comparing total energies of the nonmagnetic (NM), FM, and AFM configurations [$c(2\times2)$-AFM]. Here, the main problem is the large number of possible magnetic configurations (including the noncollinear ones) to be considered. Instead of a brute-force search, we evaluate the total energy of the disordered local moment (DLM) state similarly to Ref. 10. The DLM state is a model state with zero total magnetic moment which results from the disorder of spin orientations of otherwise nonzero local magnetic moments.[19] A strong indicator for a more complex magnetic state of the system under consideration is a lower total energy of the DLM state as compared to the NM and FM states. One should note, however, that if some specific magnetic state is the ground state, e.g., the $c(2\times2)$-AFM, its total energy is usually lower than that of the DLM state. On the other hand, in random magnetic systems, noncollinear states can be the ground state as found, e.g., in fcc-NiMn alloys[20] or in (Cu,Ni)MnSb Heusler alloys.[21] The usefulness of the DLM concept was demonstrated recently for both overlayer studies[10] and disordered magnetic semiconductors.[22] The DLM picture may be straightforwardly implemented in the framework of the coherent-potential approximation (CPA).[22] Therefore in a third step, we perform studies based on the Green's function implementation of the TB-LMTO-CPA method[23] in the framework of the surface Green's function (SGF) approach, in addition to the above mentioned collinear WIEN2K and VASP calculations. The TB-LMTO-SGF approach employs a realistic semi-infinite sample geometry (no slabs or periodic supercells) and allows to implement the DLM model. The one-electron potentials are treated within the atomic sphere approximation; the dipole barrier due to the sample electrons in the vacuum is included in the formalism. TB-LMTO-SGF even allows to include the effect of layer relaxations,[10] provided, they are known either from full-potential calculations or from experiment. An important advantage of the TB-LMTO-SGF approach is the possibility to estimate exchange interactions between magnetic atoms in the overlayer by a straightforward generalization of the well-approved bulk concept.[15,24] Summarizing, the TB-LMTO-SGF approach is a very useful tool for a qualitative understanding of the results while the full-potential approaches are superior concerning the quantitative values and thus provide so to say the corner stones. We will demonstrate that at least in the present case the results of both types of calculations are in a good quantitative agreement which justifies our assumptions and reinforces our conclusions.

II. COMPUTATIONAL DETAILS

First-principles density-functional theory calculations were performed using both the all-electron full potential linearized augmented plane wave (FP LAPW) code WIEN2K and the Vienna *ab initio* simulation package (VASP),[17] using the projector augmented wave scheme.[18] In the FP LAPW calculations the Fe/Ir(001) systems were modeled by the eleven-layer repeated slab with ≈10 Å vacuum in between. All slabs were symmetric with respect to the middle layer. We allowed the relaxations for top three layers, the remaining interlayer distances were fixed to the bulk values of 1.92 Å. For VASP repeated asymmetric slabs with seven layers Ir and a single Fe monolayer on one side and also symmetric slabs with eleven substrate layers and Fe monolayers on both sides were used, which were separated by at least 19 Å vacuum. All layer distances have been relaxed, and turned out to be essentially the same for both setups. Two DFT potential approximations have been employed: the local density approximation[25] (LDA) and the generalized gradient approximation[26] (GGA) for WIEN2K; the GGA according to Perdew and Wang (PW91) (Ref. 27) as well as the LDA as given by Perdew-Zunger[28] (Ceperley-Alder)[29] for VASP. We have tested NM-, FM-, and $c(2\times2)$-AFM magnetic arrangements, all performed in the $c(2\times2)$ structure for a reliable comparison of total energies. Technically, we have used a Brillouin zone sampling with 21–36 special k points in the irreducible two-dimensional wedge. The difference between input and output charge density in the final iteration was better than 0.1 me a.u.$^{-3}$. The total force on single atoms was in every case smaller than 1mRy/bohr.

In all TB-LMTO-SGF calculations the LDA approximation and experimental layer relaxations[11] were used. The vacuum above the overlayer was simulated as usual by empty spheres (ES). Electronic relaxations were allowed in four empty spheres adjoining the overlayer, the overlayer itself, and in five adjoining Ir substrate layers. This finite system was sandwiched self-consistently between a frozen semi-infinite fcc-Ir(001) bulk and the ES vacuum space including the dipole surface barrier. Additionally to NM-, FM-, and $c(2\times2)$-AFM configurations, we have studied DLM arrangements.

In the framework of the TB-LMTO-SGF method the exchange integrals $J_{i,j}^{\mathrm{Fe,Fe}}$ between sites i,j in the magnetic overlayer may be expressed as follows:[15,24]

TABLE I. Calculated (LDA/GGA, WIEN, and VASP, respectively) and experimental (Ref. 11) (LEED) interlayer distances d_{ij} between top three sample layers (1-Fe overlayer, 2-top Ir layer, 3-s Ir layer) for fcc-Fe/Ir(001) in the NM, FM, and $c(2\times2)$-AFM states. H_b AFM displays the influence of 0.5 ML hydrogen adsorbed on favorable bridge positions. The interlayer (001) distance in the bulk iridium is 1.92 Å.

		d_{12} (Å)		d_{23} (Å)		d_{34} (Å)	
d_{ij}		LDA	GGA	LDA	GGA	LDA	GGA
NM	WIEN	1.52	1.61	1.95	2.00	1.86	1.93
	VASP	1.51	1.58	1.99	2.05	1.88	1.94
FM	WIEN	1.64	1.78	1.91	1.95	1.88	1.94
	VASP	1.60	1.76	1.94	1.98	1.89	1.97
AFM	WIEN	1.59	1.69	1.93	1.98	1.88	1.93
	VASP	1.55	1.66	1.97	2.02	1.88	1.94
H_b-AFM	VASP	1.58	1.67	1.97	2.01	1.88	1.94
LEED		1.69		1.96		1.91	

$$J_{i,j}^{\mathrm{Fe,Fe}} = \frac{1}{4\pi}\mathrm{Im}\int_C \mathrm{tr}_L[\Delta_i^{\mathrm{Fe}}(z)g_{i,j}^{\uparrow}(z)\Delta_j^{\mathrm{Fe}}(z)g_{j,i}^{\downarrow}(z)]dz. \quad (1)$$

Here, the trace extends over s,p,d,f basis set, the quantities Δ_i^{Fe} are proportional to the calculated exchange splittings, and the Green's function $g_{i,j}^{\sigma}$ describes the propagation of electrons of a given spin ($\sigma=\uparrow,\downarrow$) between sites i,j. It should be noted that both the direct propagation of electrons in the magnetic overlayer and the indirect one via the Ir substrate are included in Eq. (1) on an equal footing. Finally, the energy integration extends over all occupied valence states up the Fermi energy E_F which is technically performed by integrating over the contour C in the complex energy plane. For more details see Ref. 15. Once the exchange interactions were known, we constructed a two-dimensional (2D) classical Heisenberg Hamiltonian to describe the magnetic behavior of the Fe overlayer on a nonmagnetic fcc-Ir(001) substrate

$$H = -\sum_{i\neq j} J_{ij}^{\mathrm{Fe,Fe}}\mathbf{e}_i\cdot\mathbf{e}_j. \quad (2)$$

In Eq. (2), $\mathbf{e}_i$ denotes the orientation of the Fe magnetic moment at the site i. By construction, the value of the corresponding magnetic moment is included in the definition of $J_{ij}^{\mathrm{Fe,Fe}}$, and positive (negative) values denote FM (AFM) couplings. An early study of exchange interactions in fcc-Fe, Co/Cu(001) systems is found in Ref. 3, whereas some recent estimates of exchange integrals for a bcc-Fe/W(001) overlayer were obtained either by a supercell approach[10,30] or by an approach closely related to the present one.[31,32]

A Green's function approach such as the present one to calculate exchange interactions has a particular advantage over a supercell approach:[10,30] Exchange interactions can be evaluated easily and reliably even for disordered overlayers and partial coverages.

III. RESULTS AND DISCUSSION

A. Structure and magnetism

The results of the total energy calculations are summarized in Tables I–IV. In Table I we present results of the structural minimization and compare our results with experiment. We found that the ground state is antiferromagnetic and that the interlayer distances obtained for this order in GGA approximation agree very well with the results of

TABLE II. Calculated work functions Φ in eV for Ir(001) (neglecting a possible lateral reconstruction) and of Fe/Ir(001) in various magnetic states. Symbols Ir, NM, FM, AFM, DLM, H_b AFM, and H_b FM denote, respectively, the Ir(001) surface, and nonmagnetic, ferromagnetic, $c(2\times2)$-antiferromagnetic, and disordered local moment states of the Fe/Ir(001) overlayer, as well as the FM and AFM states with 0.5 ML hydrogen adsorbed on bridge positions. The values correspond to the respective calculated relaxed geometries (see Table I) for WIEN/VASP, and to the experimental one (Ref. 11) for LMTO. The experimental value for the Ir(001) surface is 5.67 eV (Ref. 33).

Φ (eV)	Ir	NM	FM	AFM	DLM	H_b FM	H_b AFM
WIEN-GGA	5.65	4.86	4.38	4.45			
VASP-GGA	5.62	4.82	4.29	4.37		4.71	4.65
WIEN-LDA	5.92	5.14	4.58	4.66			
VASP-LDA	5.89	5.13	4.59	4.66		5.01	5.04
LMTO-LDA	6.22	5.05	4.79	4.76	4.67		

TABLE III. Calculated stabilities (in mRy/Fe atom) of the various magnetic phases of Fe/Ir(001) as obtained by the WIEN, VASP, and LMTO codes for the unrelaxed geometry ($d_{\text{Fe-Ir}}$=1.92 Å). The ferromagnetic ground state has the lowest energy and serves as the point of reference.

Δ (mRy)	NM_{LDA}	AFM_{LDA}	DLM_{LDA}	NM_{GGA}	AFM_{GGA}
WIEN	49.1	2.2		62.7	2.2
VASP	44.5	3.8		60.4	3.9
LMTO	42.5	5.1	2.1		

LEED structure analysis.[11] For all calculations we used the experimental lattice constant a=3.84 Å in layers, which lies between the calculated LDA bulk value (3.81 Å) below and the GGA (3.87 Å) above. For this reason, the calculated substrate interlayer distances are slightly underestimated in LDA (≈0.04 Å) and overestimated in GGA (≈0.03 Å), as the system tries to keep its respective equilibrium volume. The magnetic state influences the equilibrium surface geometry considerably at the Fe/Ir interface, while the changes in the substrate are less pronounced. A possible contamination with hydrogen, due to the preparation process should be hard to detect, as the hydrogen-induced changes in the spacings are rather small and around the experimental error limit. The differences for first interlayer distance between the FM and $c(2\times2)$-AFM configurations amount to ≈0.10 Å, while the NM Fe/Ir spacing is even smaller by 0.08 Å. The calculated top layer relaxations (about 12%) is smaller than the one obtained for the similar bcc-Fe/W(001) system (about 14 %–19 %).[9]

The first Ir-Ir distance is slightly expanded with respect to its bulk value, where one has to keep in mind that the bulk spacing is enhanced for GGA and decreased for LDA. The next spacing is reduced leading to an oscillatory pattern of interlayer distances found in many metallic systems.

The calculated work functions are presented in Table II. The experimental value of 5.7 eV for the fcc-Ir(001) is reasonably reproduced by the present calculations (no surface reconstruction). Our calculations show that the iron overlayer reduces the sample work function by ≈1 eV (no experimental data have been found). Hydrogen adsorbed on the overlayer should increase the work function by ≈0.4 eV. The calculated values for the overlayers are close to the work function of bcc Fe (about 4.5 eV) obtained for a polycrystalline sample.[33] While the full potential VASP and WIEN codes agree very well with each other, the TB-LMTO-SGF approach slightly overestimates the values.

The results of magnetic stability calculations are presented in Tables III–V. Different theoretical approaches were used and compared in tables for the unrelaxed geometry (Table III) as well as for the realistic, relaxed case (Table IV) including the possibility of residual adsorbed hydrogen (Table V). It should be noted that one may only compare different LDA or GGA energies directly to each to other. Our calculations clearly show, that the nonmagnetic case can be safely excluded. All models with local magnetic moments have a substantially lower total energy. The most striking result, obtained by all methods, is the fact that while the FM is the ground state for an unrelaxed geometry, the layer relaxations stabilize the $c(2\times2)$-AFM phase. This is in a striking contrast to the closely related bcc-Fe/W(001) case[7,8] where the antiferromagnetism of bcc-Fe/W(001) is robust with respect to the structural relaxations. Interestingly adsorbed hydrogen also does not change the picture as evident from Table V. Differences only get smaller, but the general trend is preserved. However, strictly speaking, the $c(2\times2)$ AFM may not be the true ground state of fcc-Fe/Ir(001). Similar to bcc-Fe/W(001) one should consider other possibilities, e.g., the $p(2\times1)$ AFM or even some noncollinear configurations, such as spin spirals or a chiral state.[1] To shed some light on this issue we included in Tables III and IV the results of DLM calculations as performed in the framework of the TB-LMTO-SGF approach. The sufficient reliability of the TB-LMTO-SGF approach for the present purpose is confirmed by a comparison with accurate full potential calculations for NM-, FM-, and $c(2\times2)$-AFM configurations in both the ideal and relaxed geometries. This also justifies the use of the TB-LMTO-SGF approach to obtain exchange interactions in the Fe overlayer in the following. It is quite obvious that, if the DLM state is the ground state compared to the NM and FM states, then a more complex, AFM-like state can exist and this conclusion can be reached without performing calculations for many possible candidates. But

TABLE IV. Calculated stabilities (in mRy/Fe atom) of the various magnetic phases of Fe/Ir(001) as obtained by the WIEN, VASP, and LMTO codes for relaxed geometries. The stabilities correspond to the respective calculated relaxed geometries (see Table I) for WIEN/VASP, and to the experimental one (Ref. 11) for LMTO. The antiferromagnetic ground state has the lowest energy and serves as the point of reference.

Δ (mRy)	NM_{LDA}	FM_{LDA}	DLM_{LDA}	NM_{GGA}	FM_{GGA}
WIEN	25.8	7.8		38.4	5.3
VASP	22.1	8.6		38.7	5.5
LMTO	27.7	5.0	0.8		

TABLE V. Influence of 0.5 ML adsorbed hydrogen on the calculated stabilities (in mRy) of the various magnetic phases of Fe/Ir(001) as obtained by VASP for relaxed geometries (see Table I). The antiferromagnetic ground state has the lowest energy and serves as the point of reference.

Δ (mRy)	NM_{LDA}	FM_{LDA}	NM_{GGA}	FM_{GGA}
Clean	22.1	8.6	38.7	5.5
Bridge H	14.4	3.7	29.5	2.4

clearly, this fact does not render the necessity of searching for the true ground state of the system obsolete, but rather represents a reliable qualitative indicator for a more complex magnetic state of the system.

One can speculate about the structural origin of such an AFM order. As already mentioned, both bcc(001) and fcc(001) have a common square-lattice structure of magnetic atoms which differ by the ratio $d:a_L$, where a_L is the lateral lattice constant and d is the layer spacing. For bcc(001) we have $d=a_L/2=a/2$ (where a is the bulk lattice constant) while for fcc(001) $d=a/2$ and $a_L=a/\sqrt{2}$ leading to a larger $d:a_L$. The reduction in the $d:a_L$ ratio stabilizes the AFM/DLM state for this fcc(001) surface. This ratio is sufficiently small for comparable bcc(001) surfaces even in the unrelaxed geometry [see e.g., Fe/W(001)[8]]. It is well known that the exchange interaction between Mn spins becomes antiferromagnetic for smaller distances, a trend we observe here for exchange interactions in the Fe overlayer as detailed below. This is a first strong indication that indirect interactions of Fe spins via the Ir substrate play an essential role for the fcc-Fe/Ir(001) magnetism. A dominant character of indirect interactions as compared to direct ones between Fe spins in the overlayer will result in a strong dependence of exchange interactions on the Fe-Ir interlayer distance as we shall see below.

B. Densities of states and exchange interactions

In Fig. 1 we present the layer-resolved densities of states (DOSs) for the various magnetic states. Compared to the Ir bulk, the most important feature observed for all cases is an extra contribution to the overlayer DOS around the Fermi energy due to the minority Fe states. The large exchange splitting of majority and minority Fe states is due to the enhanced overlayer magnetic moment (about $2.65\mu_B$ in all cases) which illustrates the rigidity of the Fe moment with respect to changing spin orientations. The large Fe moment is due to the large lateral overlayer lattice constant as given by the Ir substrate as well as to the reduction in coordination number at the surface typical for overlayer systems. There is also a relevant extra peak in the DOS in the vacuum close to the sample surface which gives a possibility to detect it in STM measurements. We also observe a strong reduction in the Fe-overlayer imprint on the deeper Ir-substrate layers: already the second Ir-substrate layer is almost bulklike. There is a small induced moment on the first-substrate Ir layer of the order of 0.1 μ_B while other induced moments

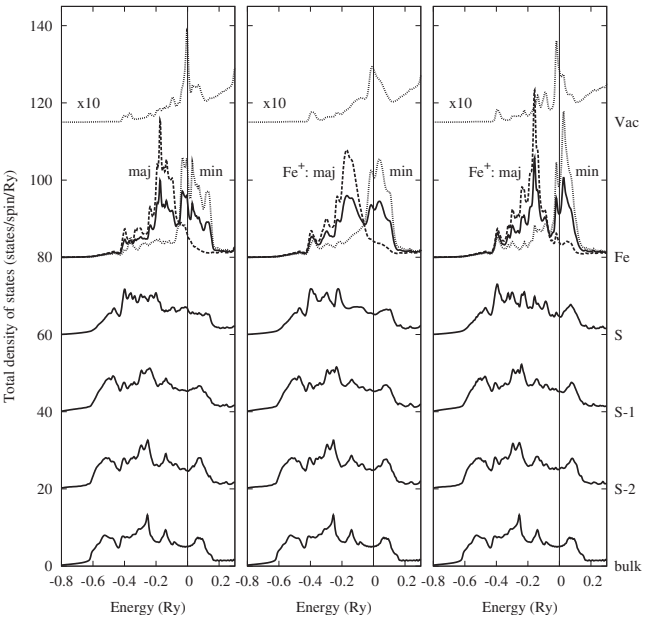

FIG. 1. Total layer-resolved DOSs for the fcc-Fe/Ir(001) overlayer and experimental layer relaxations (Ref. 11) based on the LMTO approach. In the case of the Fe overlayer the total DOSs are additionally split into majority (dashed lines) and minority (dotted lines) contributions: (a) the FM case, (b) the DLM case, and (c) the $c(2\times2)$-AFM case. Only one spin orientation (denoted as Fe^+) is plotted for the DLM and AFM cases. Symbols Vac, Fe, S-1, S-2, and bulk denote the first vacuum layer, Fe overlayer, first and second substrate Ir layers, and the fcc bulk Ir host DOSs, respectively. The Fermi energy is shifted to the energy zero.

are strongly damped in an oscillatory manner (the Friedel-type oscillations) into the Ir substrates and their values are of the order of 0.01 μ_B and smaller. It should be noted that induced moments in the Ir substrate and in the vacuum are much smaller and more strongly damped in both substrate and vacuum for the $c(2\times2)$-AFM case as compared to the FM case, while they even collapse to zero for the DLM state. The induced moment in the substrate/vacuum are more than two times smaller as those in the bcc-Fe/W(001).[10] The above results are confirmed by full-potential slab-model calculations using both WIEN and VASP codes.

Exchange interactions $J^{Fe,Fe}(d)$ have been determined by the TB-LMTO-SGF method for Fe/Ir(001) as a function of the interatomic Fe-Fe distance d for both unrelaxed and relaxed geometries, and FM-, DLM-, and AFM-reference states. Additionally we present results in the DLM state for a simple layer-relaxation model where only the Fe-Ir interlayer distance is reduced from the unrelaxed value (1.92 Å) to values of 1.82 Å, 1.72 Å, and 1.62 Å corresponding to a reduction of 5%, 10.5%, and 16%. These results are shown in Fig. 2.

Calculated exchange integrals are rather similar, e.g., all leading to the AFM interactions for the relaxed case irrespective of the reference state. The problem of the choice of reference state for estimate of exchange integrals in the present context was also addressed in Ref. 34. We have chosen the DLM reference state [with self-consistently calculated spin-polarized potentials and with corresponding modi-

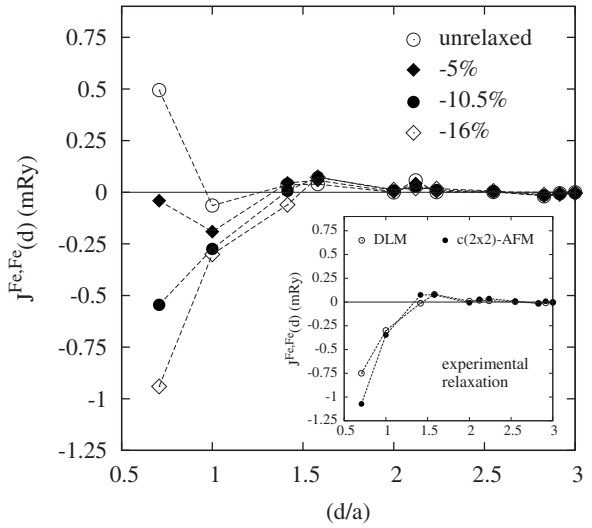

FIG. 2. Exchange interactions among Fe atoms in the Fe/Ir(001) overlayer for the unrelaxed case and model layer relaxations evaluated as a function of the reduced interatomic distance (d/a), where a denotes the lattice constant. Numbers attached to symbols indicate the reduction in the Fe-Ir interlayer distances in % as compared to the bulk value of 1.92 Å. The inset shows exchange interactions for AFM and DLM state for the experimental layer relaxations (Ref. 11). All results were obtained assuming the DLM-reference state.

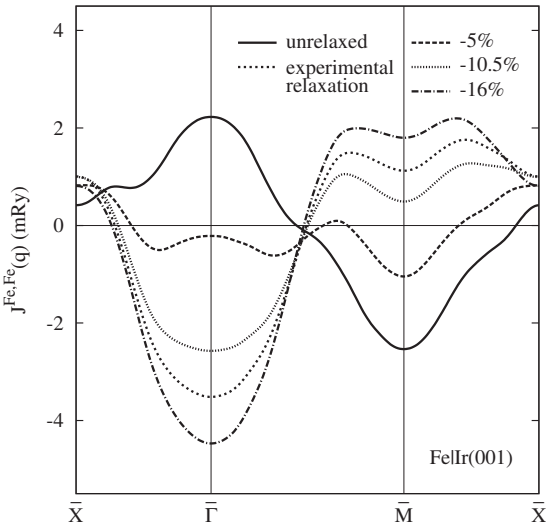

FIG. 3. Lattice Fourier transformation of the real-space exchange interactions $J_{ij}^{Fe,Fe}$, $J(\mathbf{q}_\parallel)$, for the ideal unrelaxed geometry, the experimental layer relaxations (Ref. 11) as well as for three model Fe-Ir layer relaxations (same as in Fig. 2) which were obtained for the reference DLM state of the Fe/Ir(001) overlayer. Here, $\mathbf{q}_\parallel=\bar{X}=2\pi/a_L(1/2,1/2)$, $\mathbf{q}_\parallel=\bar{\Gamma}=2\pi/a_L(0,0)$, and $\mathbf{q}_\parallel=\bar{M}=2\pi/a_L(1,0)$.

fication of Eq. (1)] for the magnetic stability study below as it assumes no magnetic ordering and for our purposes is thus most suitable. We admit that to estimate, e.g., the critical temperatures other choices may be more suitable.

With increasing layer relaxations we observe a clear tendency toward dominating AFM interactions which stabilize the AFM-like state in the overlayer. The dominating role of indirect interactions between Fe atoms via the Ir substrate is obvious: the only varying quantity is the Fe-Ir distance and thus the Fe-Ir hybridization. Results for experimental layer relaxations (inset in Fig. 2) are between model cases of 1.72 Å and 1.62 Å. The fact that strong AFM coupling in the layer-relaxed case were obtained from a reference FM state indicates the robustness of the AFM order (more precisely, of a more complex magnetic state) for the relaxed Fe/Ir(001) overlayer.

To further investigate this point we present in Fig. 3 the result of the lattice Fourier transformation of exchange integrals (1) as obtained for the DLM reference state. It should be noted that the DLM state is neither the ground state for the ideal geometry nor for the experimental layer-relaxed model. On the other hand, possible magnetic phases of 2D-Heisenberg model (2) can be obtained by studying its stability with respect to the periodic excitations. A similar approach was successfully used in the study of the complex magnetic stability of bcc Eu: starting from the FM reference state, a proper spin-spiral ground state was obtained in good agreement with the experiment.[35] Due to the sign convention in Eq. (2) the maximum of $J(\mathbf{q}_\parallel)$ corresponds to the ground state (the energy minimum). It is obvious that the ground state for the unrelaxed model is the ferromagnetic state [the maximum of $J(\mathbf{q}_\parallel)$ is obtained for $\mathbf{q}_\parallel=2\pi/a_L(0,0)$]. With reduced Fe-Ir interlayer distance we observe a quick decrease in the stability of the FM state and the ground state is found for the ordering vector $\mathbf{q}_\parallel=2\pi/a_L(1/2,1/2)$ which corresponds to the $c(2\times2)$-AFM state (for the Fe-Ir interlayer distance $d=1.82$ Å or reduced by 5%). If the Fe-Ir interlayer distance further decreases (by 10.5% and 16%) the stability of the FM state further decreases and a new, complex spin-spiral-like magnetic state becomes more stable as compared to the $c(2\times2)$-AFM state (ordering vector on the line $\bar{X}$-$\bar{M}$ in the irreducible surface Brillouin zone). On the other hand, the $c(2\times2)$-AFM state becomes more and more stable as compared to the FM state in accordance with the total-energy calculations. Also, both for the experimental layer-relaxation model[11] and for the model with the largest reduction in the Fe-Ir interlayer distance (by 16%) the $p(2\times1)$-AFM state [the ordering vector $\mathbf{q}_\parallel=2\pi/a_L(1,0)$] has lower energy as compared to the FM- and $c(2\times2)$-AFM states.

In order to advance the understanding of the present substrate induced coupling a comparison with an otherwise similar 4d substrate would be beneficial. Rhodium, crystallizes also in the fcc structure, has the same number of valence electrons [Eq. (9)] as iridium and a similar lattice constant (3.80 Å), while the value of the work function, 5.11 eV,[36] is smaller as well as the spatial extent of the 4d wave functions of Rh as compared to 5d wave functions of Ir. The results of a similar study of the magnetic stability for fcc-Fe/Rh(001) overlayer as a function of the Fe-Rh interlayer distance will be presented in the following. The same relative interlayer reductions as for fcc-Fe/Ir(001), namely, by 5%, 10.5%, and 16% will be used.

The results are summarized in Fig. 4. The FM state is again the ground state for the unrelaxed case, and we observe a similar Fe-Rh interlayer distance reduction effect on the magnetic stability as for fcc-Fe/Ir(001). The reduction in the

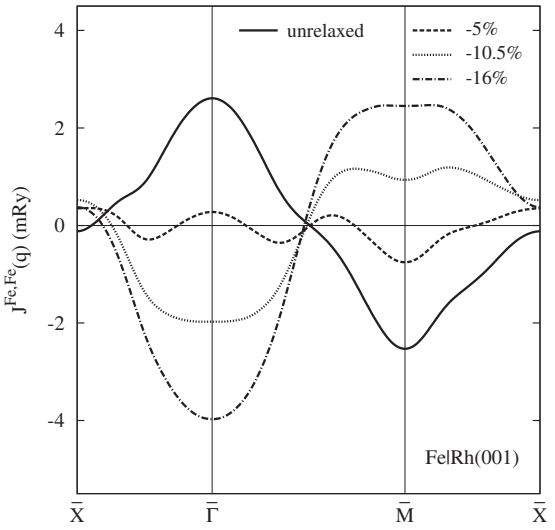

FIG. 4. Lattice Fourier transformation of real-space exchange interactions $J_{ij}^{\mathrm{Fe,Fe}}$, $J(\mathbf{q}_{\parallel})$, for the unrelaxed geometry, and three model Fe-Rh interlayer relaxations for the fcc-Fe/Rh(001) system. The identical relative interlayer distances were used for both the fcc-Fe/Ir(001) system and for the DLM reference state.

Fe-Rh interlayer distance by about 5% seems to be the point where the FM state is no longer the ground state and the $c(2\times2)$-AFM state is stabilized [the ordering vector $\mathbf{q}_{\parallel}=2\pi/a_L(1/2,1/2)$]. However, with increasing reduction in the Fe-Rh distance the more complex AFM state is stabilized until for an interlayer reduction of 16% this state become the ground state (see an indication of this case in the Fig. 4: maximum in the neighborhood of the $\mathbf{q}_{\parallel}=2\pi/a_L(1,0)$ ordering vector representing the $p(2\times1)$-AFM state). Again the AFM state is stabilized but for a relatively larger reduction in the Fe-Rh interlayer distance as compared to fcc-Fe/Ir(001), but otherwise there is a large similarity between the two overlayer systems. The larger reduction is in agreement with previous total energy study.[13]

IV. CONCLUSIONS

We have investigated the experimentally prepared Fe/Ir(001) system by a combination of different first-principles methods for both supercell slab geometries (WIEN and VASP codes) and semi-infinite boundary conditions (TB-LMTO-SGF codes). Using the latter approach we investigated the magnetic phase stability of the system by calculating the exchange interactions between Fe atoms in the overlayer. The following conclusions can be drawn. (i) Calculated relaxed geometries agree well with available experimental data. A better agreement is obtained for the Fe-Ir distance using GGA rather than LDA potentials. The calculated geometries depend on the magnetic state (nonmagnetic, FM, and AFM states) but the most important result is the reduction in the Fe-Ir interlayer distance as compared to the bulk value by about 12% for the AFM order. A possible residual H contamination on the overlayer has practically no effect on the distances. (ii) The local Fe moment is enhanced to about $2.65\mu_B$ as compared to its canonical value of $2.15\mu_B$ in the bcc Fe metal. The enhancement is due to both the enlarged lateral lattice constant of the Fe overlayer on fcc-Ir(001) and the reduction in nearest neighbors there. The work function of the system with Fe overlayer is reduced more than 1 eV as compared to the value found for pure Ir surface. Hydrogen on the overlayer increases the work function by ≈0.4 eV. (iii) Both full potential supercell methods found the $c(2\times2)$-AFM state to be stable as compared to the nonmagnetic and ferromagnetic states for the correctly relaxed structure. On the other hand, they find an FM ground state for an unrelaxed geometry. Hence, the stability of the AFM state is induced by the substrate via layer relaxations. The above results were confirmed both qualitatively and quantitatively by the TB-LMTO-SGF approach assuming a semi-infinite sample geometry and experimental layer relaxations as obtained in LEED. (iv) The related fcc-Fe/Rh(001) system behaves similarly to fcc-Fe/Ir(001), although the tendency toward the formation of the AFM state upon reduction in the Fe-Rh interlayer distance is weaker. We found an indication that a $p(2\times1)$-AFM state is stabilized for larger reductions in Fe-Rh interlayer distances. (v) A detailed study of the magnetic stability based on the 2D-Heisenberg Hamiltonian derived from the first-principles total energies confirms the stability of the $c(2\times2)$-AFM state as compared to the FM for relaxed model but indicates that more complex, spin-spiral-like state can be stabilized by reducing the Fe-Ir interlayer distance. Since Ir is a heavy element, the spin-orbit interaction can have non-negligible effect on the exchange interactions (in analogy to the Mn/W case[1]), and can lead to chiral magnetic order induced by Dzyaloshinskii-Moriya interaction. (vi) We have shown that increasing Fe-Ir hybridization stabilizes the AFM state. This seems to be a robust effect to warrant similar stabilization on a much more complex reconstructed Ir(001) surface. However, such a study goes beyond the subject of the present paper.

Experimentally no magnetization was found for iron overlayers thinner than ≈4 monolayers on fcc-Ir(001)[11] and ≈6 monolayers on fcc-Rh(001).[13] Our study indicates that this is not the result due to disappearing of the local iron magnetic moments in the top surface layers but rather due to a more complex "antiferromagneticlike" order in the fcc-iron overlayer.

ACKNOWLEDGMENTS

This work has been done within the project AV0Z1-010-0520 and AV0Z2-041-0507 of the ASCR. The authors acknowledge fruitful discussions with J. Kirschner, D. Sander, and Z. Tian and the support from the Grant Agency of the Czech Republic under Contracts No. 202/07/0456, No. 202/09/0775 and No. COST P19-OC-09028 project.

*kudrnov@fzu.cz

[1] P. Ferriani, K. von Bergmann, E. Y. Vedmedenko, S. Heinze, M. Bode, M. Heide, G. Bihlmayer, S. Blügel, and R. Wiesendanger, Phys. Rev. Lett. **101**, 027201 (2008).
[2] M. Ondráček, J. Kudrnovský, and F. Máca, Surf. Sci. **601**, 4261 (2007).
[3] M. Pajda, J. Kudrnovský, I. Turek, V. Drchal, and P. Bruno, Phys. Rev. Lett. **85**, 5424 (2000).
[4] V. S. Stepanyuk, A. N. Baranov, D. V. Tsivlin, W. Hergert, P. Bruno, N. Knorr, M. A. Schneider, and K. Kern, Phys. Rev. B **68**, 205410 (2003).
[5] P. Hyldgaard and M. Persson, J. Phys.: Condens. Matter **12**, L13 (2000).
[6] R. Wu and A. J. Freeman, Phys. Rev. B **45**, 7532 (1992).
[7] D. Spišák and J. Hafner, Phys. Rev. B **70**, 195426 (2004).
[8] A. Kubetzka, P. Ferriani, M. Bode, S. Heinze, G. Bihlmayer, K. von Bergmann, O. Pietzsch, S. Blügel, and R. Wiesendanger, Phys. Rev. Lett. **94**, 087204 (2005).
[9] P. Ferriani, S. Heinze, G. Bihlmayer, and S. Blügel, Phys. Rev. B **72**, 024452 (2005).
[10] P. Ferriani, I. Turek, S. Heinze, G. Bihlmayer, and S. Blügel, Phys. Rev. Lett. **99**, 187203 (2007).
[11] V. Martin, W. Meyer, C. Giovanardi, L. Hammer, K. Heinz, Z. Tian, D. Sander, and J. Kirschner, Phys. Rev. B **76**, 205418 (2007).
[12] Z. Tian, D. Sander, and J. Kirschner, Phys. Rev. B **79**, 024432 (2009).
[13] C. Hwang, A. K. Swan, and S. C. Hong, Phys. Rev. B **60**, 14429 (1999).
[14] J. Kudrnovský, I. Turek, V. Drchal, F. Máca, P. Weinberger, and P. Bruno, Phys. Rev. B **69**, 115208 (2004).
[15] I. Turek, J. Kudrnovský, V. Drchal, and P. Bruno, Philos. Mag. **86**, 1713 (2006).
[16] P. Blaha, K. Schwarz, G. K. H. Madsen, D. Kvasnicka, and J. Luitz, WIEN2k, *An Augmented Plane Wave Plus Local Orbitals Program for Calculating Crystal Properties* (Karlheinz Schwarz, Technische Universitat Wien, Austria, 2001).
[17] G. Kresse and J. Furthmüller, Phys. Rev. B **54**, 11169 (1996); http://cms.mpi.univie.ac.at/vasp/
[18] G. Kresse and D. Joubert, Phys. Rev. B **59**, 1758 (1999).
[19] J. Staunton, B. L. Gyorffy, A. J. Pindor, G. M. Stocks, and H. Winter, J. Phys. F: Met. Phys. **15**, 1387 (1985).
[20] H. Akai and P. H. Dederichs, Phys. Rev. B **47**, 8739 (1993).
[21] J. Kudrnovský, V. Drchal, I. Turek, and P. Weinberger, Phys. Rev. B **78**, 054441 (2008).
[22] H. Akai, Phys. Rev. Lett. **81**, 3002 (1998).
[23] I. Turek, V. Drchal, J. Kudrnovský, M. Šob, and P. Weinberger, *Electronic Structure of Disordered Alloys, Surfaces, and Interfaces* (Kluwer, Boston, 1997); I. Turek, J. Kudrnovský, and V. Drchal, in *Electronic Structure and Physical Properties of Solids*, Lecture Notes in Physics Vol. 535, edited by H. Dreyssé (Springer, Berlin, 2000), p. 349.
[24] A. I. Liechtenstein, M. I. Katsnelson, V. P. Antropov, and V. A. Gubanov, J. Magn. Magn. Mater. **67**, 65 (1987).
[25] J. P. Perdew and Y. Wang, Phys. Rev. B **45**, 13244 (1992).
[26] J. P. Perdew, A. Ruzsinszky, G. I. Csonka, O. A. Vydrov, G. E. Scuseria, L. A. Constantin, X. Zhou, and K. Burke, Phys. Rev. Lett. **100**, 136406 (2008).
[27] Y. Wang and J. P. Perdew, Phys. Rev. B **44**, 13298 (1991).
[28] J. P. Perdew and A. Zunger, Phys. Rev. B **23**, 5048 (1981).
[29] D. M. Ceperley and B. J. Alder, Phys. Rev. Lett. **45**, 566 (1980).
[30] M. Hortamani, L. Sandratskii, P. Kratzer, I. Mertig, and M. Scheffler, Phys. Rev. B **78**, 104402 (2008).
[31] L. Udvardi, A. Antal, L. Szunyogh, Á. Buruzs, and P. Weinberger, Physica B **403**, 402 (2008).
[32] A. B. Shick, F. Máca, M. Ondráček, O. N. Mryasov, and T. Jungwirth, Phys. Rev. B **78**, 054413 (2008).
[33] H. L. Skriver and N. M. Rosengaard, Phys. Rev. B **46**, 7157 (1992).
[34] L. Szunyogh and L. Udvardi, Philos. Mag. B **78**, 617 (1998).
[35] I. Turek, J. Kudrnovsky, M. Divis, P. Franek, G. Bihlmayer, and S. Blügel, Phys. Rev. B **68**, 224431 (2003).
[36] K. Christmann, Surf. Sci. Rep. **9**, 1 (1988).